

# NAS-FCOS: Fast Neural Architecture Search for Object Detection\*

Ning Wang<sup>1</sup>, Yang Gao<sup>1</sup>, Hao Chen<sup>2</sup>, Peng Wang<sup>1</sup>, Zhi Tian<sup>2</sup>, Chunhua Shen<sup>2</sup>

<sup>1</sup>School of Computer Science, Northwestern Polytechnical University, China

<sup>2</sup>School of Computer Science, The University of Adelaide, Australia

## Abstract

*The success of deep neural networks relies on significant architecture engineering. Recently neural architecture search (NAS) has emerged as a promise to greatly reduce manual effort in network design by automatically searching for optimal architectures, although typically such algorithms need an excessive amount of computational resources, e.g., a few thousand GPU-days. To date, on challenging vision tasks such as object detection, NAS, especially fast versions of NAS, is less studied.*

*Here we propose to search for the decoder structure of object detectors with search efficiency being taken into consideration. To be more specific, we aim to efficiently search for the feature pyramid network (FPN) as well as the prediction head of a simple anchor-free object detector, namely FCOS [20], using a tailored reinforcement learning paradigm. With carefully designed search space, search algorithms and strategies for evaluating network quality, we are able to efficiently search more than 2,000 architectures in around 30 GPU-days. The discovered architecture surpasses state-of-the-art object detection models (such as Faster R-CNN, RetinaNet and FCOS) by 1 to 1.9 points in AP on the COCO dataset, with comparable computation complexity and memory footprint, demonstrating the efficacy of the proposed NAS for object detection.*

## 1 Introduction

Object detection is one of the fundamental tasks in computer vision, and has been researched extensively. In the past few years, state-of-the-art methods for this task are based on deep convolutional neural networks (such as Faster R-CNN [16], RetinaNet [8]), due to their impressive performance. Typically, the designs of object detection networks are much more complex than those for image classification, because the former need to localize and classify multiple objects in an image simultaneously while the latter only need to output image-level labels. Due to its complex structure and numerous hyper-parameters, designing effective object detection networks is more challenging and usually needs much manual effort. In particular, a pyramid of feature representations are usually required to accommodate objects across a wide range of scales, which is done by a so-called Feature Pyramid Network (FPN) that takes in multi-scale feature maps from backbone CNN models and generates feature pyramids by combining the inputs from

different layers. There has been a large variety of FPN structures proposed in recent works, such as [4, 7, 11, 22]. As there are many possible choices of cross-scale connections and feature integration operations, the design space of FPN architectures can be enormous. It is very challenging to manually design an optimal FPN architecture for specific tasks.

On the other hand, Neural Architecture Search (NAS) approaches [4, 14, 26] have been showing impressive results on automatically discovering top-performing neural network architectures in large-scale search spaces. Compared to manual designs, NAS methods are data-driven instead of experience-driven, and hence need much less human intervention. As defined in [3], the workflow of NAS can be divided into the following three processes: 1) sampling architecture from a search space following some search strategies; 2) evaluating the performance of the sampled architecture; and 3) updating the search strategy based on the performance.

One of the main problems prohibiting NAS from being used in more realistic applications is its search efficiency. The evaluation process is the most time consuming part because it involves a full training procedure of a neural network. To reduce the evaluation time, in practice a proxy task is often used as a lower cost substitution. In the proxy task, the input, network parameters and training iterations are often scaled down to speedup the evaluation. However, there is often a performance gap for samples between the proxy tasks and target tasks, which makes the evaluation process biased. How to design proxy tasks that are both accurate and efficient for specific problems is a challenging problem. Another solution to improve search efficiency is constructing a supernet that covers the complete search space and training candidate architectures with shared parameters [12]. However, this solution leads to significantly increased memory consumption and restricts itself to small-to-moderate sized search spaces.

To our knowledge, studies on efficient and accurate NAS approaches to object detection networks are rarely touched, despite its significant importance. To this end, we present a fast and memory saving NAS method for object detection networks, which is capable of discovering top-performing architectures within significantly reduced search time. Our overall detection architecture is based on FCOS [20], a simple anchor-free one-stage object detection framework, in which the feature pyramid network and prediction head are searched using our proposed NAS method.

Our main contributions are summarized as follows.

- In this work, we propose a fast and memory-efficient NAS method for object detection networks, with care-

\*NW, YG, HC contributed to this work equally.

fully designed proxy tasks, search space and evaluation strategies, which is able to find top-performing architectures over 2,000 architectures using 30 GPU-days only.

Specifically, this high efficiency is enabled with the following designs.

- Employing an efficient anchor-free one-stage detection framework with simple post processing;
  - Developing a fast proxy task training scheme by caching powerful pre-trained backbone features;
  - Using a more discriminative criterion for evaluation of searched architectures.
- We empirically demonstrate that the performance of the recently introduced anchor-free one-stage detector FCOS can be considerably improved with the automatically discovered feature pyramid architecture. We term the discovered architecture NAS-FCOS.
  - We show that the overall structure of NAS-FCOS is general and flexible in that it can be equipped with various backbones including MobileNetV2, ResNet-50, ResNet-101 and ResNeXt-101, and surpasses state-of-the-art object detection algorithms using comparable computation complexity and memory footprint. More specifically, our model can improve the AP by  $1.0 \sim 1.9$  points on all above models comparing to their FCOS counterparts.

## 2 Related Work

### 2.1 Object Detection

The frameworks of deep neural networks for object detection can be roughly categorized into two types: one-stage detectors [9] and two-stage detectors [16].

Two-stage detection frameworks first generate class-independent region proposals using a region proposal network (RPN), and then classify and refine them using extra detection heads. In spite of achieving top performance, the two-stage methods have noticeable drawbacks: they are computationally expensive and have many hyper-parameters that need to be tuned to fit a specific dataset.

In comparison, the structures of one-stage detectors are much simpler. They directly predict object categories and bounding boxes at each location of feature maps generated by a single CNN backbone.

Note that most state-of-the-art object detectors (including both one-stage detectors [9, 13, 15] and two-stage detectors [16]) make predictions based on anchor boxes of different scales and aspect ratios at each convolutional feature map location. However, the usage of anchor boxes may lead to high imbalance between object and non-object examples and introduce extra hyper-parameters. More recently, anchor-free one-stage detectors [20, 24], have attracted increasing research interests, due to their simple fully convolutional architectures and reduced consumption of computational resources.

### 2.2 Neural Architecture Search

NAS is usually time consuming. We have seen great improvements from 24,000 GPU-days [26] to 0.2 GPU-day [23]. The trick is to first construct a supernet containing the complete search space and train the candidates all at once with bi-level optimization and efficient weight sharing [12]. It has been applied to semantic segmentation search [10] but the large memory allocation and difficulties in approximated optimization prohibit the search for more complex structures.

Recently researchers [1, 5, 19] propose to apply single-path training to reduce the bias introduced by approximation and model simplification of the supernet. DetNAS [2] follows this idea to search for an efficient object detection architecture. One limitation of the single-path approach is that the search space is restricted to a sequential structure. However, single-path sampling and straight through estimate of the weight gradients introduce large variance to the optimization process and prohibit the search for more complex structures under this framework. Within this very simple search space, NAS algorithms can only make trivial decisions like kernel sizes for manually designed modules. One can hardly observe any design insights from the search results.

Object detection models are different from single-path image classification networks in their way of merging multi-level features and distributing the task to parallel prediction heads. Feature pyramid network (FPN) [8], designed to handle this job, plays an important role in modern object detection models. NAS-FPN [4] targets on searching for an FPN alternative based on one-stage framework RetinaNet [9]. Feature pyramid architectures are sampled with A recurrent neural network (RNN) controller. The RNN controller is trained with reinforcement learning (RL). However, the search takes 8K TPU-hours even though a proxy task with ResNet-10 backbone is trained to evaluate each architecture, which is not affordable by most practitioners.

To speed up reward evaluation of RL-based NAS, the work of [14] proposes to use progressive tasks and other training acceleration methods. By caching the encoder features, they are able to train semantic segmentation decoders with very large batch sizes very efficiently. In the sequel of this paper, we refer to this technique as fast decoder adaptation. However, directly applying this technique to object detection tasks does not enjoy similar speed boost, because they are either not in using a fully-convolutional model [8] or require complicated post processing that are not scalable with the batch size [9].

To reduce the post processing overhead, we resort to a recently introduced anchor-free one-stage framework, namely, FCOS [20]. In our exploratory experiments, *we found that the processing time of anchor-box matching in RetinaNet can take as much as 50% of the entire search time.* Compared to its anchor-based counter part, FCOS significantly reduces the training memory footprint while being able to improve the performance. Different from NAS-FPN, we also include the prediction head in our search space. Note that our proposed approach is orders of magnitude faster than NAS-FPN [4] in terms of search efficiency.

### 3 Our Approach

In our work, we use anchor-free fully convolutional detection models with fast decoder adaptation. Thus, NAS methods can be easily applied.

#### 3.1 Problem Formulation

We base our search algorithm upon a one-stage framework FCOS because of its simplicity. Our training tuples  $\{(\mathbf{x}, Y)\}$  consist of input image tensors  $\mathbf{x}$  of size  $(3 \times H \times W)$  and FCOS output targets  $Y$  in a pyramid representation, which is a list of tensors  $\mathbf{y}_l$  each of size  $((K + 4 + 1) \times H_l \times W_l)$  where  $H_l \times W_l$  is feature map size on level  $p$  of the pyramid.  $(K + 4 + 1)$  is the output channels of FCOS, the three terms are length- $K$  one-hot classification labels, 4 bounding box regression targets and 1 centerness factor respectively.

The network  $g : \mathbf{x} \rightarrow \hat{Y}$  in original FCOS consists of three parts, a backbone  $b$ , FPN  $f$  and multi-level subnets we call prediction heads  $h$  in this paper. First backbone  $b : \mathbf{x} \rightarrow C$  maps the input tensor to a set of intermediate-leveled features  $C = \{c_3, c_4, c_5\}$ , with resolution  $(H_i \times W_i) = (H/2^i \times W/2^i)$ . Then FPN  $f : C \rightarrow P$  maps the features to a feature pyramid  $P = \{p_3, p_4, p_5, p_6, p_7\}$ . Then the prediction head  $h : p \rightarrow y$  is applied to each level of  $P$  and the result is collected to create the final prediction. To avoid overfitting, same  $h$  is often applied to all instances in  $P$ .

Since different scale objects requires different effective receptive fields, the mechanism to select and merge intermediate-leveled features  $C$  is particularly important in object detection network design. Thus, most researches [13, 16] are carried around designing  $f$  and  $h$  while using widely-adopted backbone structures such as ResNet [6]. Following this principle, our search goal is to decide when to choose which features from  $C$  and how to merge them.

Similar to [14], we reuse the parameters in  $b$  pretrained on target dataset and search for the optimal structures after that. Following the nomenclature in that paper, we call the network components to search for,  $f$  and  $h$ , together the decoder structure for the objection detection network.

$f$  and  $h$  take care of different parts of the detection job.  $f$  extracts features targeting different object scales in the pyramid representations  $P$ . While  $h$  is a unified mapping applied to each feature in  $P$  to avoid overfitting. In practice, people seldom discuss the possibility of using a more diversified  $f$  to extract features at different levels or how many layers in  $h$  need to be shared across the levels. To use NAS as an automatic method to test these possibilities, we design our search space with the following two questions in mind:

- How to provide flexibility for structures and operation options to generate the feature pyramid?
- How to balance the workload between  $f$  and  $h$ ?

#### 3.2 Search Space

The building block for our decoder is similar to [14]. We replace the cell structure with atomic operations to provide

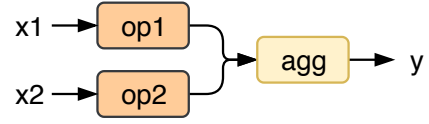


**Figure 1** – Basic building block of NAS-FCOS. Two operations  $op1$ ,  $op2$  are applied to two specified features at  $id1$ ,  $id2$  and then the outputs are aggregated by  $agg$ . If the two features have different sizes, the smaller one is scaled up via bilinear upsampling to match the larger one.

ID	Description
0	separable conv $3 \times 3$
1	separable conv $3 \times 3$ with dilation rate 3
2	separable conv $5 \times 5$ with dilation rate 6
3	skip-connection
4	deformable $3 \times 3$ convolution

**Table 1** – Description of unary operations used in the search process.

even more flexibility. To construct one basic block, we first choose two layers  $x_1, x_2$  from the sampling pool  $X$  at  $id1$ ,  $id2$ , then two operations  $op1$ ,  $op2$  are applied to each of them and an aggregation operation  $agg$  merges the two output into one feature. The structure of the basic block is shown in Fig. 1. To build a deep decoder structure, we apply multiple basic blocks with their outputs added to the sampling pool. Our basic block  $bb_t : X_{t-1} \rightarrow X_t$  at time step  $t$  transforms the sampling pool  $X_{t-1}$  to  $X_t = X_{t-1} \cup \{x_t\}$ , where  $x_t$  is the output of  $bb_t$ .

We rely on a similar set of operations as for semantic segmentation [14] (Table 1). We include only separable/depth-wise convolutions so that the decoder can be efficient. In order to enable the decoder to apply convolutional filters on irregular grids, here we have also included deformable  $3 \times 3$  convolutions [25]. We will explore the possibility of adding depth-wise deformable convolutions to the search space in future work. For the aggregation operations, we include element-wise sum and concatenation followed by a  $1 \times 1$  convolution.

The decoder configuration can be represented by a sequence with three components, FPN configuration, head configuration and weight sharing stages. We provide detailed descriptions to each of them in the following sections. The complete diagram of our decoder structure is shown in Fig. 2.

##### 3.2.1 FPN Search Space

As mentioned above, FPN  $f$  maps the convolutional features  $C$  to  $P$ . First, we initialize the sampling pool as  $X_0 = C$ . Our FPN is defined by applying the basic block 7 times to the sampling pool,  $f := bb_1^f \circ bb_2^f \circ \dots \circ bb_7^f$ . To yield pyramid features  $P$ , we collect the last three basic block outputs  $\{x_5, x_6, x_7\}$  as  $\{p_3, p_4, p_5\}$ .

To allow shared information across all layers, we use a simple rule to create global features. If there is some dangling layer  $x_t$  which is not sampled by later blocks  $\{bb_i^f | i > t\}$  nor belongs to the last three layers  $t < 5$ , we

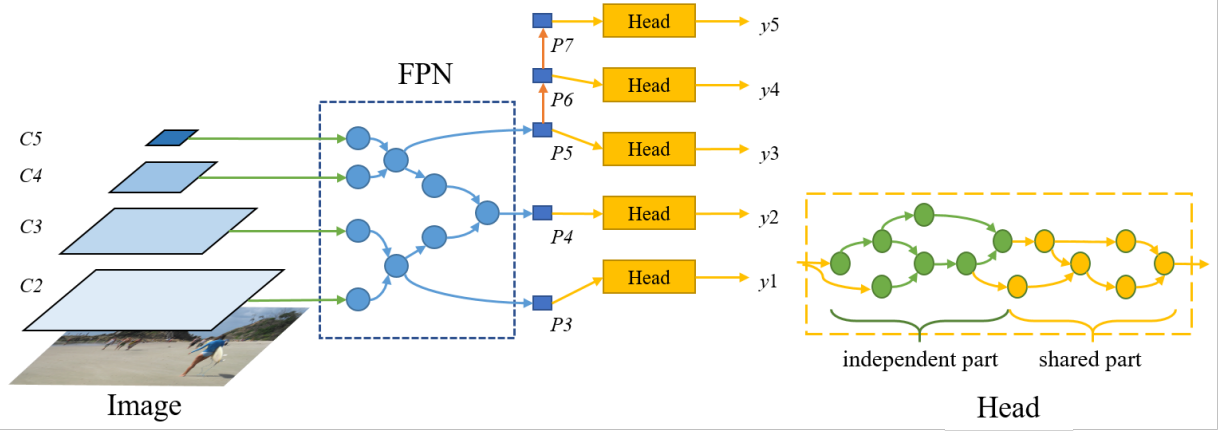


**Figure 2** – A conceptual example of our NAS-FCOS decoder. It consists of two sub networks, an FPN  $f$  and a set of prediction heads  $h$  which have shared structures. One notable difference with other FPN-based one-stage detectors is that our heads have partially shared weights. Only the last several layers of the predictions heads (marked as yellow) are tied by their weights. The number of layers to share is decided automatically by the search algorithm. Note that both FPN and head are in our actual search space; and have more layers than shown in this figure. Here the figure is for illustration only.

use element-wise add to merge it to all output features

$$\mathbf{p}_i^* = \mathbf{p}_i + \mathbf{x}_t, \quad i \in \{3, 4, 5\}. \quad (1)$$

Same as the aggregation operations, if the features have different resolution, the smaller one is upsampled with bilinear interpolation.

To be consistent with FCOS,  $\mathbf{p}_6$  and  $\mathbf{p}_7$  are obtained via a  $3 \times 3$  stride-2 convolution on  $\mathbf{p}_5$  and  $\mathbf{p}_6$  respectively.

### 3.2.2 Prediction Head Search Space

Prediction head  $h$  maps each feature in the pyramid  $\mathbf{p}$  to the output of corresponding  $\mathbf{y}$ . Instead of using a sequential search space similar to FCOS prediction towers, we simply modify the FPN search space for head generation. There are two notable differences:

1. A single operation is applied to the input  $\mathbf{p}$  without any aggregation operator, its output  $\mathbf{o}_0$  together with  $\mathbf{p}$  is set to be the initial sampling pool,  $X_0 = \{\mathbf{p}, \mathbf{o}_0\}$ ;
2. After that, basic block  $bb^h$  is repeated five times,  $h := bb_1^h \circ bb_2^h \circ \dots \circ bb_5^h$ ;
3. Within these basic blocks, outputs of each operation  $\mathbf{o}$  along with their aggregation result  $\mathbf{a}$  are added into the sampling pool,  $X_t = X_{t-1} \cup \{\mathbf{o}_t^1, \mathbf{o}_t^2, \mathbf{a}_t\}$ .

The final output of the head is the aggregation output of the last (fifth) basic block  $\mathbf{a}_t$ . An example of the head structure with its complete search space is illustrated in Fig. 3.

### 3.2.3 Searching for Head Weight Sharing

To add even more flexibility and understand the effect of weight sharing in prediction heads, we further add an index  $i_l$  to each level  $l$ , indicating the starting layer for the prediction head  $h_l$  to share weights with the others. In this way, we enable each head to decide how many stages it would like to share features with the others. For every layer before this stage, the head  $h_l$  will create its own set of weights, otherwise, it will use the global weights.

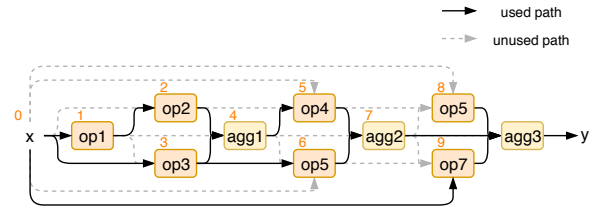


**Figure 3** – Example head structure of the decoder. The digit at the upper left corner of each operator is the index of the intermediate features. The head is designed to utilize these features by skip connections. Except the first operator, other operators can be connected from any previous outputs. The solid black lines indicate the used paths and dashed grey lines are other unused possible paths. The head configuration to generate the above head is  $[\text{op1}, [1, 0, \text{op2}, \text{op3}, \text{agg1}], [4, 3, \text{op4}, \text{op5}, \text{agg2}], [2, 0, \text{op6}, \text{op7}, \text{agg3}]]$ .

We can consider the independent part of the heads as extended FPN branch and the shared part as head with adaptive-length. In this way, we can further balance the workload for each individual FPN branch to extract level-specific features and the prediction head shared across all levels.

### 3.3 Search Strategy

Similar strategy as [14] is applied to the search process. We rely on an LSTM-based controller to predict the full configuration. The training dataset is randomly split into a meta-train  $D_t$  and meta-val  $D_v$  subset. To speed up the training, we fix the backbone network and cache the pre-computed backbone output  $C$ . This makes our single architecture training cost independent from the depth of backbone network. Taking this advantage, we can apply much more complex backbone structures and utilize high quality multilevel features as our decoder’s input. Speedup techniques such as Polyak weight averaging are also applied during the training.

The most widely used detection metric is average precision (AP). However, because of the difficulty of the task, at the early stages, AP is too low to tell the good architectures

from the bad ones. To make the architecture evaluation process easier even at the early stages of the training, we use negative loss sum as the reward instead of average precision:

$$R(a) = - \sum_{(x,Y) \in D_v} (L_{cls}(x, Y|a) + L_{reg}(x, Y|a) + L_{ctr}(x, Y|a)),$$

where  $L_{cls}$ ,  $L_{reg}$ ,  $L_{ctr}$  are the three loss terms in FCOS.

Gradient of the controller is estimated via proximal policy optimization (PPO) [18].

## 4 Experiments

### 4.1 Searching Implementation Details

For the search process, our decoders are trained on PASCAL VOC, which contains 5715 images with object bounding box annotations of 20 classes. We first train our backbone network, ResNet-50 with FPN and FCOS head as the decoder on VOC. The backbone network is initialized with pretrained weights provided by open-source implementation of FCOS<sup>1</sup>. Then it is fine-tuned on VOC using input resolution  $1330 \times 800$  with batch size 24 and crop size  $800 \times 800$ . The model is trained for 30K iterations with initial learning rate 0.01. We reduce our learning rate to one tenth at the 18K-th and 24K-th iteration.

We design a fast proxy task for decoder architecture evaluation. The VOC training set is randomly splitted into a meta-train set with 4,000 images and a meta-val set with 1715 images. We pre-compute the backbone features with input images resized to short size 384 then randomly cropped to  $384 \times 384$ . Target object sizes of interest are scaled correspondingly. All operations in the decoder have 64 output channels. The decoder inputs  $C$  are first resized to fit this channel width with  $1 \times 1$  convolutions. We use Adam optimizer with learning rate  $8e-4$  and batch size 200. Polyak averaging is applied with the decay rates of 0.9. The decoder is evaluated after 15 epochs.

### 4.2 Training Implementation Details

The controller model is nearly converged after searching about 2.8K architectures on the proxy task. Then, the top-20 best performing architectures sampled by the RL controller during the proxy task are selected for full training purpose.

We train our detection models on MS COCO, which contains 115K training images and 5K validation images. Our training setting is similar to FCOS' original one. Input images are resized to short size 800, the maximum long side is set to be 1333. The models are trained with batch size 16 for 90K iterations. The initial learning rate is 0.01 and reduced to one tenth at the 60K-th and 80K-th iteration.

<sup>1</sup><https://tinyurl.com/FCOSv1>

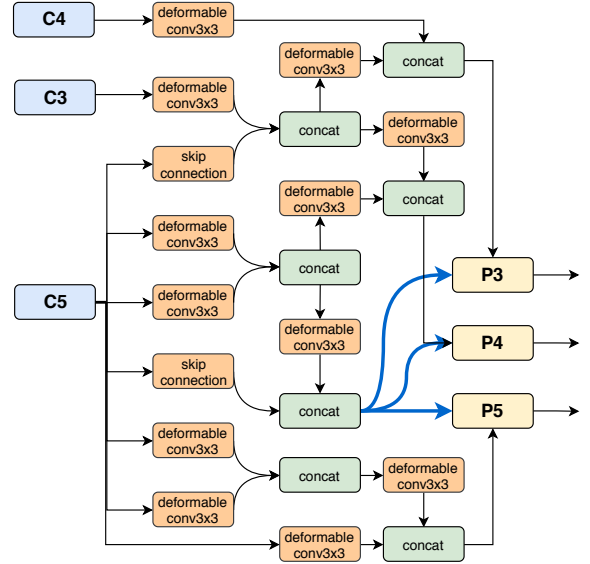


**Figure 4** – Our discovered FPN structure.  $C_2$  is omitted from this figure because it is not sampled by our decoder.

### 4.3 Search Results

The best FPN structure is illustrated in Fig. 4. The controller can identify that deformable convolution and concatenation are the best performing operations for unary and aggregation respectively.

We use the searched decoder together with either lightweight backbones such as MobileNet-V2 [17] or more powerful backbones such as ResNet-101 [6] and ResNeXt-101 [21]. To balance the performance and efficiency, we implement three decoders with different computation budgets: one with feature dimension of 128 (@128), one with 256 (@256), another with FPN channel width 128 and prediction head 256 (@128-256). The results on the COCO test-dev with short side being 800 is shown in Table 2. The searched decoder with feature dimension of 256 (@256) surpasses its FCOS counterpart by 1 to 1.9 points in AP under different backbones. The One with 128 channels (@128) has significantly reduced parameters and calculation with a slight precision drop, making it more suitable for resource-constrained environments. The third type of decoder (@128-256) achieves a good balance between accuracy and parameters. The comparison of FLOPs and number of parameters with other models are illustrated in Fig. 5 and Fig. 6 respectively. By adjusting the number of channels in the searched decoder, our model shows its flexibility in balancing precision and computational budgets.

We also demonstrate the comparison with other NAS methods for object detection in Table 3. Our NAS method is able to search for twice more architectures than DetNAS [2] using less GPU resources. Note that the AP of NAS-FPN [4] is achieved by stacking the searched FPN 7 times, while we do not stack our searched FPN.

### 4.4 Ablation Study

#### 4.4.1 Design of reinforcement learning reward

The use of reward functions is important in the standard reinforcement learning framework. As we discussed in 3.3, it

Decoder	Backbone	FLOPs (G)	Params (M)	AP
FPN-RetinaNet @256	MobileNetV2	133.4	11.3	30.8
FPN-FCOS @256	MobileNetV2	105.4	9.8	31.2
NAS-FCOS (ours) @128	MobileNetV2	<b>39.5</b>	<b>7.7</b>	30.6
NAS-FCOS (ours) @128-256	MobileNetV2	105.6	12.3	32.2
NAS-FCOS (ours) @256	MobileNetV2	131.8	23.7	<b>33.1</b>
<hr/>				
FPN-RetinaNet @256	R-50	198.0	33.6	36.1
FPN-FCOS @256	R-50	169.9	32.0	37.4
Deformable-FPN-FCOS @256	R-50	172.2	35.1	37.9
NAS-FCOS (ours) @128	R-50	<b>104.3</b>	<b>29.6</b>	37.2
NAS-FCOS (ours) @128-256	R-50	170.4	34.1	38.3
NAS-FCOS (ours) @256	R-50	199.6	46.0	<b>38.9</b>
<hr/>				
FPN-RetinaNet @256	R-101	262.4	52.5	37.8
FPN-FCOS @256	R-101	<b>234.3</b>	<b>50.9</b>	41.5
NAS-FCOS (ours) @256	R-101	264.0	64.9	<b>42.5</b>
<hr/>				
FPN-FCOS @256	X-101	<b>387.7</b>	<b>94.9</b>	42.7
NAS-FCOS (ours) @256	X-101	417.4	108.9	<b>43.7</b>

**Table 2** – Results on test-dev set of MS COCO after full training. R-50 and R-101 represents ResNet backbones and X-101 represents ResNeXt-101 ( $32 \times 4d$ ). All networks share the same input resolution. FLOPs and runtime are being measured on  $1088 \times 800$ , which is the median of the input size on COCO. For RetinaNet and FCOS, we use official models provided by the authors. For our FPN-FCOS, @128 and @256 means that the decoder channel width is 128 and 256 respectively. @128-256 is the decoder with FPN width 128 and head width 256.

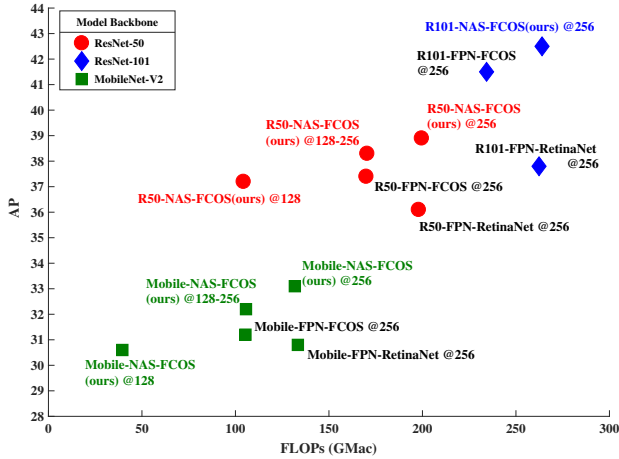


**Figure 5** – Diagram of the relationship between FLOPs and AP. Points of different shapes represent different backbones. By adjusting the number of channels, we can achieve a good balance between precision and computation. NAS-FCOS@128 has a slight decrease in precision but gains the advantage of computation quantity. One with 256 channels obtains the highest precision with more computation complexity. Using FPN channel width 128 and prediction head 256(@128-256) offers a trade-off.

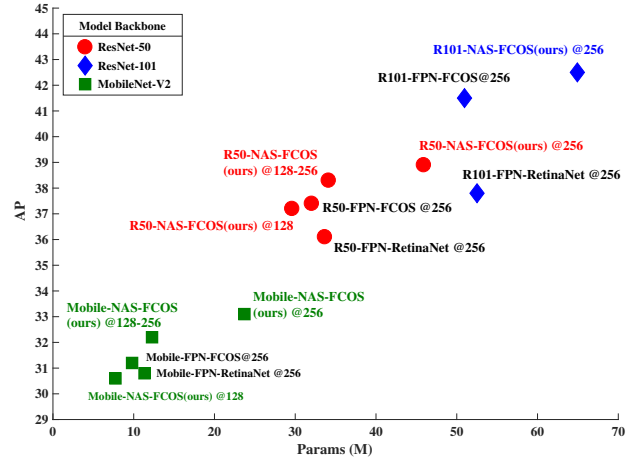


**Figure 6** – The relationship between parameters and AP with different backbones. Similar to computation, adjusting the number of channels in the FPN structure and head helps to achieve a balance between accuracy and parameters.

is a common idea to use widely accepted indicators as rewards for specific tasks in the search, such as using mIOU for semantic segmentation tasks and AP for object detection tasks. However, we found that using AP as the reward did not show a clear upward trend in short-term search rounds. We further analyze the possible reason for this situation to be that the controller RNN learns a mapping from the decoder sequence to the reward while the calculation process of AP itself is complicated, which makes it difficult to learn the mapping process within a limited number of iterations. Although researchers have demonstrated the feasibility of AP as the reward in its recent work [4], the number of itera-

tions they need to search reaches 17,000, far exceeding the 2800 iterations we need in our experiments. In view of this, we consider using the sum of classification loss, regression loss and center-ness loss [20] as the reward, which is simpler and more effective in theory. Comparative experiments in both cases showed that the loss on the validation set is better at model feedback than AP for reinforcement learning. Comparison chart is shown in Fig. 7. In the first 1,000 iterations, the trend of using validation set loss is more obvious than the one using AP. We also show the reward curve during the whole proxy task in Fig. 8, which continues to rise until almost 2,800 iterations.

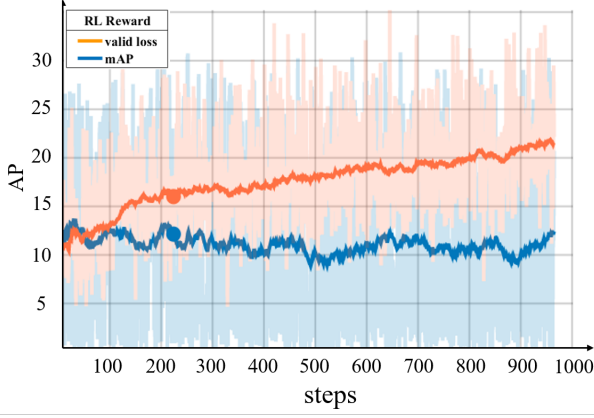


**Figure 7** – Comparison of two different RL reward designs.

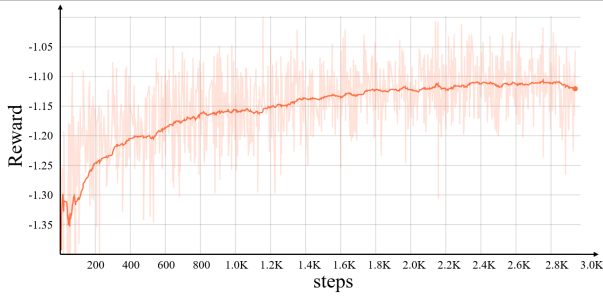


**Figure 8** – Performance of reward during the proxy task, which has been growing throughout the process, indicating that the model of reinforcement learning works.

#### 4.4.2 Selection of candidate operations

As mentioned above, deformable convolutions are included in the set of candidate operations, which are able to adapt to the geometric variations of objects. In order to control the variables, we replace the whole standard  $3 \times 3$  convolutions with deformable  $3 \times 3$  convolutions and train a Deformable-FPN-FCOS model for fair comparison. It turns out that our NAS-FCOS model still achieves better performance than the Deformable-FPN-FCOS model under this circumstance.

#### 4.4.3 Inference time

By comparing against the results reported in Table 1 of [4], the discovered model ‘NAS-FCOS @128’ using ResNet50 as the backbone appears to be competitive with YOLOv3-Darknet53 in FLOPs and AP. On a single V100 GPU card, inference time of our model NAS-FCOS @128-R50 is as follows:

- $600 \times 600$  input, 37 ms (27 FPS);
- $800 \times 800$  input, 39 ms (26 FPS);
- $1000 \times 1000$  input, 50 ms (20 FPS).

Using the MobileNetV2 as the backbone, the inference can be faster with a slight drop in AP.

## 5 Conclusion

In this paper, we have proposed to use Neural Architecture Search to further optimize the process of designing

object detection networks. It is shown in this work that top-performing detectors can be efficiently searched using carefully designed proxy tasks, search strategies and model evaluation metrics. The experiments on COCO demonstrates the efficiency of our discovered model NAS-FCOS and its flexibility to be used with various backbone architectures.

## References

- [1] H. Cai, L. Zhu, and S. Han. Proxylessnas: Direct neural architecture search on target task and hardware. *arXiv preprint arXiv:1812.00332*, 2018.
- [2] Y. Chen, T. Yang, X. Zhang, G. Meng, C. Pan, and J. Sun. DetNAS: Neural architecture search on object detection. *arXiv preprint arXiv:1903.10979*, 2019.
- [3] T. Elsken, J. H. Metzen, and F. Hutter. Neural architecture search: A survey. *arXiv preprint arXiv:1808.05377*, 2018.
- [4] G. Ghiasi, T.-Y. Lin, R. Pang, and Q. V. Le. NAS-FPN: Learning scalable feature pyramid architecture for object detection. *Proc. IEEE Conf. Comp. Vis. Patt. Recogn.*, 2019.
- [5] Z. Guo, X. Zhang, H. Mu, W. Heng, Z. Liu, Y. Wei, and J. Sun. Single path one-shot neural architecture search with uniform sampling. *arXiv preprint arXiv:1904.00420*, 2019.
- [6] K. He, X. Zhang, S. Ren, and J. Sun. Identity mappings in deep residual networks. In *European conference on computer vision*, pages 630–645. Springer, 2016.
- [7] A. Kirillov, R. Girshick, K. He, and P. Dollr. Panoptic feature pyramid networks. *arXiv: Computer Vision and Pattern Recognition*, 2019.
- [8] T.-Y. Lin, P. Dollár, R. Girshick, K. He, B. Hariharan, and S. Belongie. Feature pyramid networks for object detection. In *Proc. IEEE Conf. Comp. Vis. Patt. Recogn.*, pages 2117–2125, 2017.
- [9] T.-Y. Lin, P. Goyal, R. Girshick, K. He, and P. Dollár. Focal loss for dense object detection. In *Proc. IEEE Conf. Comp. Vis. Patt. Recogn.*, pages 2980–2988, 2017.
- [10] C. Liu, L.-C. Chen, F. Schroff, H. Adam, W. Hua, A. Yuille, and L. Fei-Fei. Auto-deeplab: Hierarchical neural architecture search for semantic image segmentation. *Proc. IEEE Conf. Comp. Vis. Patt. Recogn.*, 2019.
- [11] H. Liu, C. Peng, C. Yu, J. Wang, X. Liu, G. Yu, and W. Jiang. An end-to-end network for panoptic segmentation. In *Proc. IEEE Conf. Comp. Vis. Patt. Recogn.*, 2019.
- [12] H. Liu, K. Simonyan, and Y. Yang. Darts: Differentiable architecture search. *arXiv preprint arXiv:1806.09055*, 2018.
- [13] W. Liu, D. Anguelov, D. Erhan, C. Szegedy, S. Reed, C.-Y. Fu, and A. Berg. SSD: Single shot multibox detector. In *Proc. Eur. Conf. Comp. Vis.*, pages 21–37. Springer, 2016.

Head	Backbone	Search Cost (GPU-day)	Searched Archs	AP
NAS-FPN 7@256 [4]	R-50	$333 \times \# \text{TPUs}$	17000	<b>44.8</b>
FPN-Faster	DetNASNet [2]	44	2200	40.0
RetinaNet	DetNASNet [2]	44	2200	33.3
NAS-FCOS (ours) @256	R-50	<b>30</b>	2800	38.9
NAS-FCOS (ours) @256	R-101	<b>30</b>	2800	42.5

**Table 3** – Comparison with other NAS methods. The input size for NAS-FPN is  $1280 \times 1280$ . For NAS-FPN, the search cost should be timed by their number of TPUs used to train each architecture. Note that the accuracy of NAS-FPN here is obtained with the FPN structure being stacked 7 times. The input size for DetNASNet is not reported in the original paper.



**Figure 9** – Inference results of the NAS-FCOS model (ours) on the validation set of MS COCO dataset, together with RetinaNet and FCOS. All the models use ResNet-50 as the encoder.

- [14] V. Nekrasov, H. Chen, C. Shen, and I. Reid. Fast neural architecture search of compact semantic segmentation models via auxiliary cells. *Proc. IEEE Conf. Comp. Vis. Patt. Recogn.*, 2019.
- [15] J. Redmon and A. Farhadi. YOLOv3: An incremental improvement. *arXiv*, 2018.
- [16] S. Ren, K. He, R. Girshick, and J. Sun. Faster R-CNN: Towards real-time object detection with region proposal networks. In *Proc. Advances in Neural Inf. Process. Syst.*, pages 91–99, 2015.
- [17] M. Sandler, A. Howard, M. Zhu, A. Zhmoginov, and L.-C. Chen. Mobilenetv2: Inverted residuals and linear bottlenecks. In *Proc. IEEE Conf. Comp. Vis. Patt. Recogn.*, pages 4510–4520, 2018.
- [18] J. Schulman, F. Wolski, P. Dhariwal, A. Radford, and O. Klimov. Proximal policy optimization algorithms. *arXiv: Comp. Res. Repository*, 2017.
- [19] D. Stamoulis, R. Ding, D. Wang, D. Lymberopoulos, B. Priyantha, J. Liu, and D. Marculescu. Single-path NAS: Designing hardware-efficient convnets in less than 4 hours. *arXiv preprint arXiv:1904.02877*, 2019.
- [20] Z. Tian, C. Shen, H. Chen, and T. He. FCOS: Fully convolutional one-stage object detection. *arXiv preprint arXiv:1904.01355*, 2019.

- [21] S. Xie, R. Girshick, P. Dollr, Z. Tu, and K. He. Aggregated residual transformations for deep neural networks. *arXiv preprint arXiv:1611.05431*, 2016.
- [22] T. Zhao and X. Wu. Pyramid feature attention network for saliency detection. *arXiv: Computer Vision and Pattern Recognition*, 2019.
- [23] H. Zhou, M. Yang, J. Wang, and W. Pan. BayesNAS: A bayesian approach for neural architecture search. *arXiv preprint arXiv:1905.04919*, 2019.
- [24] C. Zhu, Y. He, and M. Savvides. Feature selective anchor-free module for single-shot object detection. *arXiv preprint arXiv:1903.00621*, 2019.
- [25] X. Zhu, H. Hu, S. Lin, and J. Dai. Deformable convnets v2: More deformable, better results. *arXiv preprint arXiv:1811.11168*, 2018.
- [26] B. Zoph and Q. V. Le. Neural architecture search with reinforcement learning. *arXiv preprint arXiv:1611.01578*, 2016.